

pH-Triggered Controlled Drug Release from Mesoporous Silica Nanoparticles via Intracellular Dissolution of ZnO Nanolids

Faheem Muhammad,^{†,§} Mingyi Guo,^{†,§} Wenxiu Qi,[‡] Fuxing Sun,[†] Aifei Wang,[†] Yingjie Guo,^{*,†} and Guangshan Zhu^{*,†}

[†]State Key Laboratory of Inorganic Synthesis and Preparative Chemistry, College of Chemistry, and [‡]College of Life Science, Jilin University, Changchun 130021, China

S Supporting Information

ABSTRACT: Acid-decomposable, luminescent ZnO quantum dots (QDs) have been employed to seal the nanopores of mesoporous silica nanoparticles (MSNs) in order to inhibit premature drug (doxorubicin) release. After internalization into HeLa cells, the ZnO QD lids are rapidly dissolved in the acidic intracellular compartments, and as a result, the loaded drug is released into the cytosol from the MSNs. The ZnO QDs behave as a dual-purpose entity that not only acts as a lid but also has a synergistic antitumor effect on cancer cells. We anticipate that these nanoparticles may prove to be a significant step toward the development of a pH-sensitive drug delivery system that minimizes drug toxicity.

In the past two decades, nanotechnology has brought about a paradigm shift in cancer therapy.¹ Since traditional anticancer drugs cannot distinguish between cancerous and healthy cells, collateral damage and adverse side effects are almost inevitable. To address this formidable challenge, diverse classes of nanoscale drug delivery systems, such as drug–polymer conjugates,² micelles, liposomes,³ dendrimers,⁴ and inorganic nanoparticles,⁵ have been developed to capitalize on enhanced permeability and retention (i.e., passive targeting) and endorse site-specific delivery. Among these nanoscopic therapeutic systems, mesoporous silica nanoparticles (MSNs)⁶ have emerged as robust nanovectors for drug delivery because of their remarkable biocompatibility and stability, among other features. The intriguing concept of stimulus-responsive gatekeeping of functionalized MSNs was introduced as a means of regulating the movement of cargo molecules. In these gated systems, a variety of capping agents, such as nanoparticles, organic molecules, and supramolecular nanovalves, have been employed as “gatekeepers” that can be maneuvered by various stimuli such as changes in redox state,^{7–10} pH,^{11–14} electrostatics,¹⁵ enzymatic activity,^{16–18} photoirradiation,^{19–22} magnetic actuation,²³ and electric field.²⁴ Upon stimulation, these gatekeepers allow the release of the cargo from the reservoir into a specific environment. Of the stimuli previously studied, changing the pH represents an effective strategy for cancer therapies because it enables exploitation of the acidic environment of cancerous tissue. It is well-documented that the pH in tumor and inflammatory tissues is more acidic than in blood and normal tissue, with endosomes and lysosomes exhibiting even lower pH values. This motivated us to design

nanocarriers that could respond to physiopathological pH signals to trigger selective drug release in cancerous cells.

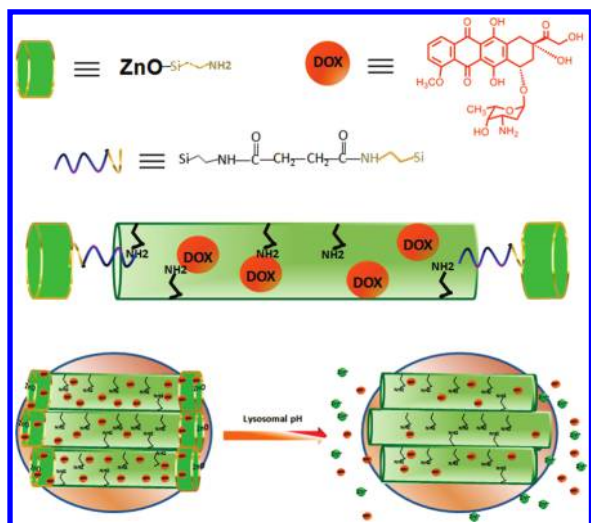
Previous studies have reported the pH-responsive capping and uncapping of MSNs by various gatekeepers, including supramolecular nanovalves, pH-sensitive linkers, and polyelectrolytes. For example, the macrocyclic molecule cucurbit[6]uril was employed to regulate the movement of cargo molecules.^{25a} Another pH-driven gate involved the anchoring of a polyamine onto the surface of the MSN.^{25b} Both systems, however, were limited by their tendency to undergo base-driven release (at pH ~10), rendering them unsuitable for biological applications. Subsequently, a few acid-responsive supramolecular nanovalves^{25c,d} and gold nanoparticle-capped MSNs that control the release of cargo molecules have been reported. Fabrication of these supramolecular nanomachines involves tedious and intricate steps, whereas the acid-labile linkers (e.g., acetal,¹⁴ boronate ester¹¹) connecting the gold nanoparticles to mesoporous silica are hydrolyzed at rather low pH (3–4), which is not appropriate for intracellular applications. To circumvent these challenges, we have developed a facile alternative system that uses acid-decomposable ZnO quantum dots (QDs) to cap MSNs (Scheme 1). The primary motivations for employing ZnO QDs as nanolids lie in the fact that they are easy to fabricate, inexpensive, and exhibit adequate response to acid (they are stable at pH 7.4 but rapidly dissolve at pH <5.5). Moreover, we have been able to demonstrate that ZnO QDs not only guard the cytotoxic drug from premature release but also themselves exhibit cytotoxic effects at their destination. The capping of ZnO QD lids on anticancer-drug-loaded MSNs should therefore allow pH-triggered drug release to improve the therapeutic index of drugs and lower their side effects.

MSNs were first synthesized according to a previously reported method.⁷ Transmission electron microscopy (TEM) (Figure 1) showed that the resulting spherical MSNs had diameters of ~100 nm and 2.1 nm wide channel-like pores. The MSNs were then selectively bifunctionalized as shown in Scheme S1 in the Supporting Information. Carboxylic groups were anchored onto the outer surfaces of the MSNs (denoted COOH–MSNs), after which the surfactant was extracted via ion exchange to preserve the organic functional groups. The inner channels of the COOH–MSNs were then partially functionalized with amines to obviate electrostatic interactions between the cationic anticancer drug doxorubicin (DOX)

Received: January 13, 2011

Published: May 17, 2011

Scheme 1. Schematic Illustration of the Synthesis of ZnO@MSNs–DOX and Working Protocol for pH-Triggered Release of the Anticancer Drug (DOX) from ZnO@MSNs–DOX to the Cytosol via Selective Dissolution of ZnO QDs in the Acidic Intracellular Compartments of Cancer Cells



($pK_a = 8.2$) and the negatively charged (Si–O) pore walls of the COOH–MSNs (Figure S3 and Table S1). A new ligand-exchange-free strategy was developed to prepare water-dispersible, luminescent ZnO QDs. Aminopropyl-functionalized ZnO QDs (denoted NH_2 –ZnO) with an average particle diameter of 3–4 nm were well-characterized by TEM, energy-dispersive spectroscopy (EDS) analysis, and FTIR spectroscopy (Figures S4 and S5). DOX, the model drug for this proof-of-concept study, was readily loaded into the pores of COOH–MSNs by incubation for 12 h. The DOX loading was determined to be as high as 0.075 mmol/g (40 mg/g). After the drug was loaded, the nanopores of the COOH–MSNs were sealed with NH_2 –ZnO QDs through amide coupling with 1-ethyl-3-(3-dimethylaminopropyl)carbodiimide (EDC).

The electron microscopy images verified the capping with ZnO, as distinctive dark, crystalline spots with diameters of 3–4 nm on the surfaces of the MSNs were observed (Figure 1a,c). These ZnO QDs (3–4 nm diameter) were large enough to block the 2.1 nm pores of the MSNs and thus inhibit the release of the loaded DOX. Wide-angle powder X-ray diffraction (XRD) patterns also indicated the presence of ZnO (Figure S1). The successful drug loading and ZnO capping of the COOH–MSNs were further confirmed by the decrease in the intensity of the (100) XRD peak (Figure S1) and the reduction in surface area (Figure S2).

In order to clearly demonstrate the acid dissolution of the ZnO QDs, the sample was subjected to TEM, scanning electron microscopy (SEM), inductively coupled plasma–optical emission spectroscopy (ICP–OES), fluorescence, and cargo-release studies. ZnO-capped MSNs (ZnO@MSNs) were incubated in acetate buffer (pH 5.0) for a few seconds, and the resultant smooth surfaces of the MSNs with their hexagonally packed mesoporous channels could clearly be seen by electron microscopy (Figure 1b,d), indicating the disintegration of ZnO. The extent of dissolution of the ZnO QDs was quantified by ICP–OES (Figure S7). After the ZnO@MSNs were incubated in phosphate-buffered saline (PBS, pH 7.4) for 48 h, dissolved

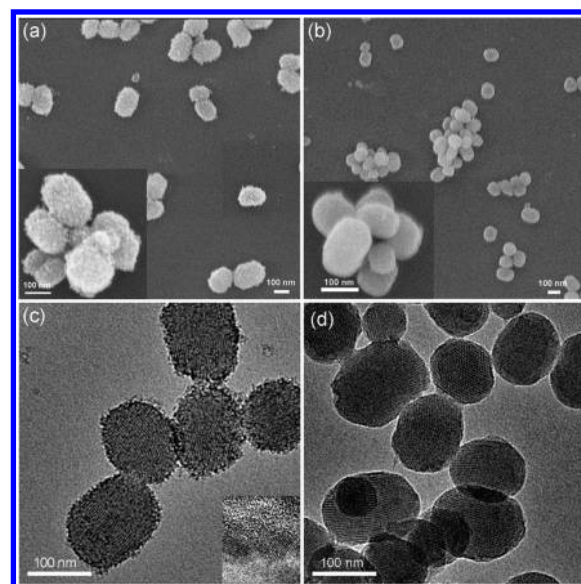


Figure 1. (a) SEM and (c) TEM micrographs of ZnO@MSNs. The inset in (c) is a high-resolution TEM image. (b) SEM and (d) TEM micrographs of the sample obtained after incubation in pH 5.0 buffer solution, showing the dissolution of the ZnO QDs.

ionic Zn^{2+} was found to account for only 2.2% of the total Zn. In contrast, after incubation of the ZnO@MSNs in acetate buffer for just 5 min, >99% of the zinc was found to be in the form of free Zn^{2+} . These findings suggested that upon internalization by cells, the ZnO QDs could readily be dissolved in acidic intracellular compartments, whereas their dissolution elsewhere in the body would be appreciably slow. Since the NH_2 –ZnO QDs were luminescent, fluorescence spectroscopy could also be used to confirm their acid-sensitive behavior. ZnO@MSNs were luminescent in PBS (pH 7.4) (Figure S4a), but this luminescence was rapidly quenched upon incubation at pH 5.0 (Figure S4b), substantiating the acid-sensitive decomposition of the ZnO capping.

To investigate the pH-triggered uncapping efficiency of DOX-loaded ZnO@MSNs (ZnO@MSNs–DOX), release experiments were performed at different pH values. Figure 2a demonstrated negligible DOX release from ZnO@MSNs–DOX at physiological pH (7.4), signifying efficient confinement of DOX in the pores of the MSNs by virtue of capping with ZnO QDs. In contrast, the fast release of DOX at pH 5.0 was consistent with dissolution of the ZnO nanolids in the acidic environment. The release reached a plateau at 0.026 mmol/g within 5 h and then remained little changed over hours due to the electrostatic interaction between DOX and the silanol groups of silica.²⁶ Although the dissolution of ZnO nanolids at pH 5.0 was confirmed in the above-mentioned studies, the drug release behavior was also studied at pH 2.0 to attenuate the electrostatic interaction between the drug molecules and the MSNs. A control experiment without ZnO caps was also carried out and revealed that ~5% (3.7 μ mol/g) of the DOX was released at pH 7.4; however, the release at pH 5.0 was found to be ~10% (7.4 μ mol/g) (Figure 2b). The significantly higher DOX release from the ZnO@MSNs–DOX sample can be ascribed to the well-reported interaction between DOX and metal ions.²⁷ During the capping step (after loading), some DOX molecules were also chemisorbed onto the ZnO QDs and instantly released

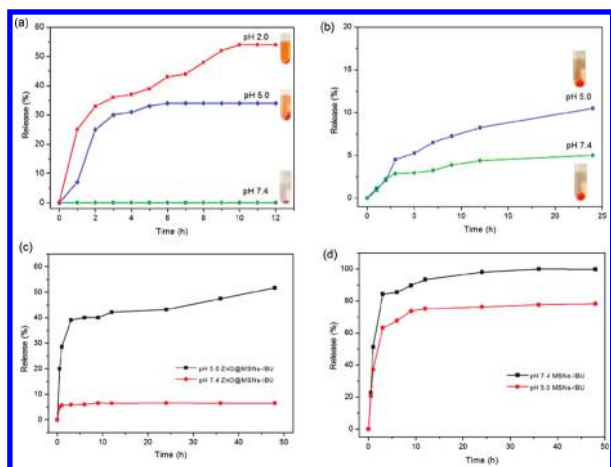


Figure 2. (a) Release profiles of ZnO@MSNs–DOX at pH 7.4, 5.0, and 2.0 at 37 °C. (b) Release profiles of MSNs–DOX at pH 7.4 and 5.0 without ZnO capping. Inset: photographs of the corresponding centrifuged MSNs samples (5 mg/mL) indicating the extent of drug release over 6 h. (c) Release profiles of ZnO@MSNs–IBU at pH 7.4 and 5.0. (d) Release profiles of MSNs–IBU at pH 7.4 and 5.0. The release of drug molecules was monitored using a UV–vis spectrophotometer.

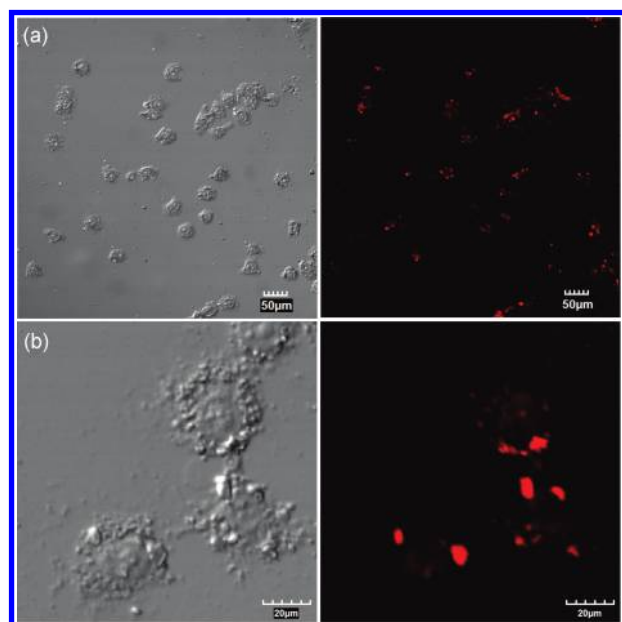


Figure 3. (a) Low- and (b) high-magnification CLSM images of HeLa cells after incubation with 100 μg/mL ZnO@MSNs–DOX for 3 h: (left) transmission images; (right) fluorescence images.

upon ZnO dissolution (Figure S8). To further validate pH-triggered controlled cargo release from ZnO@MSNs, the anionic drug ibuprofen (IBU) (100 mmol/g) and the model dye fluorescein (1.2 μmol/g) were loaded into COOH–MSNs. It can be seen from Figure 2d that the rate of IBU release from MSNs–IBU was well-controlled and that in contrast to DOX, a higher amount of drug was released at pH 7.4. Figure 2c indicates that zero release of IBU from ZnO@MSNs–IBU at pH 7.4 was observed. Once the pH was lowered, the drug was sustainably delivered over 48 h. The fluorescein-loaded sample similarly exhibited zero release over a period of 60 h at physiological pH

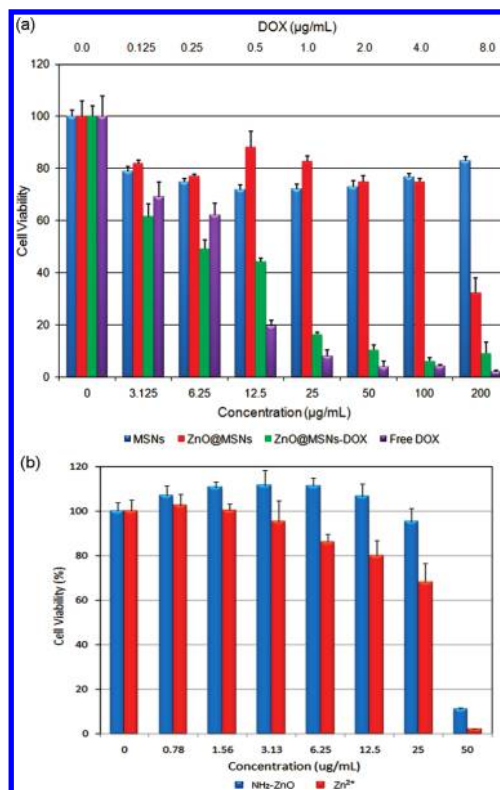


Figure 4. (a) In vitro viability of HeLa cells in the presence of COOH–MSNs, ZnO@MSNs, ZnO@MSNs–DOX, and free DOX. (b) Cell viability of ZnO QDs and comparable concentrations of Zn²⁺ ions. The incubation time was 48 h.

but ready release of the fluorescein guest molecules when the pH was decreased to 5, as shown in Figure S9.

The cellular uptake and intracellular release behaviors were investigated by confocal laser scanning microscopy (CLSM). After incubation of HeLa cells with ZnO@MSNs–DOX for 3 h, the MSNs were rapidly internalized into the cells and localized mainly in the cytoplasm and subcellular vesicles, as indicated by the clearly visible red fluorescence of DOX (Figure 3). The intracellular release of DOX was attributed to the decomposition of ZnO nanolids in the acidic lysosomal compartments, consistent with previous reports of the dissolution of ZnO nanowires because of the acidity of the lysosomes.²⁸

An MTT assay was used for quantitative testing of the viability of HeLa cells in the presence of COOH–MSNs, ZnO@MSNs, ZnO@MSNs–DOX, and free DOX. As shown in Figure 4, COOH–MSNs had no obvious effect on cell viability at concentrations up to 200 μg/mL, whereas ZnO@MSNs exhibited a statistically significant cytotoxic effect, most notably at 200 μg/mL. The half-maximal inhibitory concentration (IC₅₀) of ZnO@MSNs–DOX against HeLa cells was calculated to be ~15 μg/mL, suggesting a fairly high therapeutic effectiveness.

In order to prove the intracellular dissolution of the nanolids into Zn²⁺, we evaluated the cell viability of cancer cell lines with comparable concentrations of ZnO QDs and Zn²⁺ ions (as ZnCl₂) upon incubation for 48 h. Both samples indicated strong antitumor activity when the concentration exceeded 25 μg/mL. Taken together, these results imply that cell death could be attributed to the intracellular dissolution of ZnO QDs into ionic Zn²⁺. The cytotoxicity of Zn²⁺ has been attributed to its

induction of reactive oxygen species (ROS) production, lipid peroxidation, and DNA damage.²⁹ Furthermore, it has been reported that ZnO nanoparticles preferentially kill cancer cells because cancerous T cells exhibit higher inducible levels of ROS than normal T cells.³⁰ Consequently, ZnO QDs alone have utility as an anticancer therapeutic agent.

The viability studies also demonstrate that ZnO@MSNs—DOX greatly decreased the cell viability at concentrations as low as 6.25 $\mu\text{g/mL}$, which is comparable to the cytotoxic effect of free DOX. Unlike free DOX, however, we expect that the ZnO@MSNs to deliver the cytotoxic agent selectively to the more acidic cancerous cells than to normal tissue.

In summary, we have demonstrated that ZnO QD lids on MSNs can be efficiently dissolved in the acidic intracellular compartments of cancer cells, resulting in release of the drug cargo from the pores of the MSNs into the cytosol. In view of the therapeutic potential of ZnO QDs themselves and the acidic exterior and interior environments of cancer cells, the use of ZnO QDs to cap MSNs should prove to be a valuable pH-responsive strategy for the delivery of anticancer agents.

■ ASSOCIATED CONTENT

S Supporting Information. Experimental details and characterization data. This material is available free of charge via the Internet at <http://pubs.acs.org>.

■ AUTHOR INFORMATION

Corresponding Author

guoyingjie@jlu.edu.cn; zhugs@jlu.edu.cn

Author Contributions

⁵These authors contributed equally.

■ ACKNOWLEDGMENT

This work was financially supported by an Outstanding Young Scientist Award from the National Natural Science Foundation of China (NSFC) (20625102), the International Science and Technology Cooperation Program (2007DFA40830), NSFC grants (20831002 and 20571030), and the Jilin Province Hi-Tech Development Project (20082104).

■ REFERENCES

- (1) (a) Peer, D.; Karp, J. M.; Hong, S.; Farokhzad, O. C.; Margalit, R.; Langer, R. *Nat. Nanotechnol.* **2007**, *2*, 751. (b) Murthy, S. K. *Int. J. Nanomed.* **2007**, *2*, 129. (c) Ferrari, M. *Nat. Rev. Cancer* **2005**, *5*, 161. (d) Duncan, R. *Nat. Rev. Cancer* **2006**, *6*, 688. (e) Singh, R.; Lillard, J. W., Jr. *Exp. Mol. Pathol.* **2009**, *3*, 215.
- (2) Vicent, M. J.; Duncan, R. *Trends Biotechnol.* **2006**, *24*, 39.
- (3) Torchilin, V. P. *Nat. Rev. Drug Discovery* **2005**, *4*, 145.
- (4) Gillies, E. R.; Fréchet, J. M. J. *Drug Discovery Today* **2005**, *10*, 35.
- (5) Brown, S. D.; Nativio, P.; Smith, J.; Stirling, D.; Edwards, P. R.; Venugopal, B.; Flint, D. J.; Plumb, J. A.; Graham, D.; Wheate, N. J. *J. Am. Chem. Soc.* **2010**, *132*, 4678.
- (6) (a) Slowing, I. I.; Trewyn, B. G.; Giri, S.; Lin, V. S. Y. *Adv. Funct. Mater.* **2007**, *17*, 1225. (b) Hyeon, T.; Lee, J. E.; Lee, N.; Kim, H.; Kim, J.; Choi, S. H.; Kim, J. H.; Kim, T.; Song, I. C.; Park, S. P.; Moon, W. K. *J. Am. Chem. Soc.* **2010**, *132*, 552.
- (7) Lai, C. Y.; Trewyn, B. G.; Jeftinija, D. M.; Jeftinija, K.; Xu, S.; Jeftinija, S.; Lin, V. S.-Y. *J. Am. Chem. Soc.* **2003**, *125*, 4451.
- (8) Giri, S.; Trewyn, B. G.; Stellmaker, M. P.; Lin, V. S.-Y. *Angew. Chem., Int. Ed.* **2005**, *44*, 5038.
- (9) Kim, H.; Kim, S.; Park, C.; Lee, H.; Park, H. J.; Kim, C. *Adv. Mater.* **2010**, *22*, 4280.
- (10) Liu, R.; Zhao, X.; Wu, T.; Feng, P. *J. Am. Chem. Soc.* **2009**, *131*, 14418.
- (11) Aznar, E.; Marcos, M. D.; Martínez-Mañez, R.; Sancenón, F.; Soto, J.; Amorós, P.; Guillem, C. *J. Am. Chem. Soc.* **2009**, *131*, 6833.
- (12) Zhao, Y. L.; Li, Z.; Kabehie, S.; Botros, Y. Y.; Stoddart, J. F.; Zink, J. I. *J. Am. Chem. Soc.* **2010**, *132*, 13016.
- (13) Angelos, S.; Yang, Y.-W.; Patel, K.; Stoddart, J. F.; Zink, J. I. *Angew. Chem., Int. Ed.* **2008**, *47*, 2222.
- (14) Liu, R.; Zhang, Y.; Zhao, X.; Agarwal, A.; Mueller, L. J.; Feng, P. *J. Am. Chem. Soc.* **2010**, *132*, 1500.
- (15) Casasús, R.; Marcos, M. D.; Martínez-Mañez, R.; Ros-Lis, J. V.; Soto, J.; Villaescusa, L. A.; Amorós, P.; Beltrán, D.; Guillem, C.; Latorre, J. *J. Am. Chem. Soc.* **2004**, *126*, 8612.
- (16) Patel, K.; Angelos, S.; Dichtel, W. R.; Coskun, A.; Yang, Y. W.; Zink, J. I.; Stoddart, J. F. *J. Am. Chem. Soc.* **2008**, *130*, 2382.
- (17) Schlossbauer, A.; Kecht, J.; Bein, T. *Angew. Chem., Int. Ed.* **2009**, *48*, 3092.
- (18) Bernardos, A.; Aznar, E.; Marcos, M. D.; Martínez-Mañez, R.; Sancenón, F.; Soto, J.; Barat, J. M.; Amorós, P. *Angew. Chem., Int. Ed.* **2009**, *48*, 5884.
- (19) Mal, N. K.; Fujiwara, M.; Tanaka, Y. *Nature* **2003**, *421*, 350.
- (20) Ferris, D. P.; Zhao, Y. L.; Khashab, N. M.; Khatib, H. A.; Stoddart, J. F.; Zink, J. I. *J. Am. Chem. Soc.* **2009**, *131*, 1686.
- (21) Vivero-Escoto, J. L.; Slowing, I. I.; Wu, C.; Lin, V. S.-Y. *J. Am. Chem. Soc.* **2009**, *131*, 3462.
- (22) Lin, Q.; Huang, Q.; Li, C.; Bao, C.; Liu, Z.; Li, F.; Zhu, L. *J. Am. Chem. Soc.* **2010**, *132*, 10645.
- (23) Thomas, C. R.; Ferris, D. P.; Lee, J. H.; Choi, E.; Cho, M. H.; Kim, E. S.; Stoddart, J. F.; Shin, J. S.; Cheon, J.; Zink, J. I. *J. Am. Chem. Soc.* **2010**, *132*, 10623.
- (24) Zhu, Y.; Liu, H.; Li, F.; Ruan, Q.; Wang, H.; Fujiwara, M.; Wang, L.; Lu, G. Q. *J. Am. Chem. Soc.* **2010**, *132*, 1450.
- (25) (a) Angelos, S.; Yang, Y.-W.; Patel, K.; Stoddart, J. F.; Zink, J. I. *Angew. Chem., Int. Ed.* **2008**, *47*, 2222. (b) Casasús, R.; Climent, E.; Marcos, M. D.; Martínez-Mañez, R.; Sancenón, F.; Soto, J.; Amorós, P.; Cano, J.; Ruiz, E. *J. Am. Chem. Soc.* **2008**, *130*, 1903. (c) Park, C.; Oh, K.; Lee, S. C.; Kim, C. *Angew. Chem., Int. Ed.* **2007**, *46*, 1455. (d) Angelos, S.; Khashab, N. M.; Yang, Y.-W.; Trabolsi, A.; Khatib, H. A.; Stoddart, J. F.; Zink, J. I. *J. Am. Chem. Soc.* **2009**, *131*, 12912.
- (26) (a) Lebold, T.; Jung, C.; Michaelis, J.; Brauchle, C. *Nano Lett.* **2009**, *9*, 2877. (b) Meng, H.; Xue, M.; Xia, T.; Zhao, Y.-L.; Tamanoi, F.; Stoddart, J. F.; Zink, J. I.; Nel, A. E. *J. Am. Chem. Soc.* **2010**, *132*, 12690.
- (27) (a) Fiallo, M. M. L.; Suillerot, A. G.; Matzanke, B.; Kozlowski, H. *J. Inorg. Biochem.* **1999**, *75*, 105. (b) Kheirloomoom, A.; Mahakian, L.; Lai, C. Y.; Lindfors, H. A.; Ferrara, K. *Mol. Pharmaceutics* **2010**, *7*, 1948. (c) Abraham, S. A.; Edwards, K.; Kasrllsson, G.; MacIntosh, S.; Mayer, L. D.; McKenzie, C.; Bally, M. B. *Biochim. Biophys. Acta* **2002**, *1565*, 41.
- (28) Müller, K. H.; Kulkarni, J.; Motskin, M.; Goode, A.; Winship, P.; Skepper, J. N.; Ryan, M. P.; Porter, A. E. *ACS Nano* **2010**, *4*, 6767.
- (29) (a) Deng, X.; Luan, Q.; Chen, W.; Wang, Y.; Wu, M.; Zhang, H.; Jiao, Z. *Nanotechnology* **2009**, *20*, No. 115101. (b) Kröncke, K.-D. *Arch. Biochem. Biophys.* **2007**, *463*, 183. (c) Xia, T.; Kovochich, M.; Liong, M.; Madler, L.; Gilbert, B.; Shi, H.; Yeh, J. I.; Zink, J. I.; Nel, A. E. *ACS Nano* **2008**, *2*, 2121. (d) George, S.; Pokhrel, S.; Xia, T.; Gilbert, B.; Ji, Z. X.; Schowalter, M.; Rosenauer, A.; Damoiseaux, R.; Bradley, K. A.; Madler, L.; Nel, A. E. *ACS Nano* **2010**, *4*, 15. (e) Gazaryan, I. G.; Krasinskaya, I. P.; Kristal, B. S.; Brown, A. M. *J. Biol. Chem.* **2007**, *282*, 24373.
- (30) Hanley, C.; Layne, J.; Punnoose, A.; Reddy, K. M.; Coombs, I.; Coombs, A.; Feris, K.; Wingett, D. *Nanotechnology* **2008**, *19*, No. 295103.